Full-Wave Analysis and Modeling of Multiconductor Transmission Lines via 2-D-FDTD and Signal-Processing Techniques

Feng Liu, José E. Schutt-Ainé, *Senior Member, IEEE,* and Ji Chen, *Member, IEEE*

***Abstract*—The full-wave analysis of the multiconductor transmission lines on an inhomogeneous medium is performed by using the two-dimensional finite-difference time-domain (FDTD) method. The FDTD data are analyzed by using signal-processing techniques. The use of high-resolution signal-processing techniques allows one to extract the dispersive characteristics and normal-mode parameters, which include decoupled modal impedances and current and voltage eigenvector matrices. A new algorithm for extracting frequency-dependent equivalent-circuit parameters is presented in this paper. Smaller CPU time and memory are required as compared to the three-dimensional FDTD case. Numerical results are presented to demonstrate the accuracy and efficiency of this method.**

***Index Terms*—Frequency-dependent parameters, FDTD, transmission lines.**

I. Introduction

As THE SPEED of high-performance very large scale integration (VLSI) circuit increases, the full-wave nature of interconnections becomes important and wave aspects such as signal distortion and signal coupling between different interconnects must be considered. Recent developments in microwave integrated circuits (MICs) have also led to complex waveguide structures with multiple conductors on inhomogeneous substrate, which may or may not be anisotropic. Accurate electrical modeling of these structure is required to insure robust simulation at the design stage. This requirement can be fulfilled by a full-wave modeling approach through a solution of Maxwell's equations, which includes electromagnetic effects.

Among the available full-wave techniques, the finite-difference time-domain (FDTD) method is one of the most attractive methods. The main advantage of the FDTD technique is its ability to model arbitrary structures. Recently, some work was performed on the extraction of equivalent-circuit parameters of multiconductors by FDTD [1]–[2], [14]. However, the computational efficiency and memory requirements of these methods limit their practicality. The memory requirement stems from the three-dimensional (3-D) nature of the FDTD mesh. Only after the incident impulse has reached stability and the modes have been defined along the direction of propagation can a discrete Fourier transform be used to select the information of interest in the frequency domain.

Recently, a new two-dimensional finite-difference time-domain (2-D-FDTD) approach for frequency-selective full-wave analysis was introduced to analyze the arbitrary waveguiding structures [3]–[4]. Although the dispersive characteristics can be obtained from Fourier transformation, the modal information is not available. In some applications, this modal information is essential and must be retrieved. It has been observed that, in many microstrip simulations, the modes are formed rapidly. Due to the presence of noise, lengthy simulation time is required in order to attain higher SNR for Fourier transformation. In [10], the authors make use of the signal-processing algorithm ESPRIT as a post-processing engine to extract the broad-band modal information after the three-dimensional finite-difference time-domain (3-D-FDTD) simulation. In their approach, the ESPRIT algorithm is implemented in the spatial domain along the propagation direction, in which a huge mesh size along this dimension is required.

In this paper, we present a new approach to extract multimode parameters of guided wave structures from 2-D-FDTD simulations. In our approach, the super-resolution algorithms [5]–[6] from signal-processing techniques is employed in the temporal domain. The estimation of signal parameters via a rotational invariance technique (i.e., ESPRIT) algorithm is presented due to its robustness against white noise, which leads to shorter simulation time. In addition, the templates for the modes can be estimated accurately. This approach is based on the assumption that the computational error is additive white Gaussian noise, which is a good approximation at high frequency [10]. The resulting modal information is used to verify this new approach. Based on this approach, a new algorithm is presented to extract the frequency-dependent equivalent-circuit parameters of multiconductor transmission lines.

II. Problem Formulation

The system considered here is an arbitrary multiconductor microstrip line system in inhomogeneous media. The system is homogeneous along the direction of propagation of the wave. The substrate is lossless, but it can be anisotropic in the transverse directions. In the following discussion, z is the direction

Manuscript received February 10, 2000; revised October 16, 2000.

F. Liu was with the Department of Electrical and Computer Engineering, University of Illinois at Urbana-Champaign, Urbana, IL 61801 USA. He is now with Synopys Inc., Mountain View, CA 94043 USA (e-mail: fliu@synopsys.com).

J. E. Schutt-Ainé is with the Department of Electrical and Computer Engineering, University of Illinois at Urbana-Champaign, Urbana, IL 61801 USA (e-mail: jose@decwa.ece.uiuc.edu).

J. Chen was with the Personal Communications Systems Research Laboratories, Motorola Inc., Harvard, IL 60033 USA. He is now with the Department of Electrical and Computer Engineering, University of Houston, Houtson, TX 77204 USA (e-mail: ji.chen@mail.uh.edu).

Publisher Item Identifier S 0018-9480(02)01169-9.

of propagation, whereas x, y are the transverse directions. The system consists of N coupled transmission lines.

A. 2-D-FDTD Formulation

Due to the invariance in the direction of propagation, the phasor associated with the electromagnetic field has the form $\mathbf{A}(x, y, z) = \mathbf{A}(x, y)\exp\{\pm j\beta z\}$. Once the modes are established, a phase shift $\exp\{\pm j\beta z\}$ exists between any two adjacent nodes for a given propagation constant β [3]–[4]. It is easy to see that an incident or reflected impulse having a propagation constant β satisfies

$$\begin{aligned} E_x^n, E_y^n, H_z^n &= \{E_x^n(x,y), E_y^n(x,y), H_z^n(x,y)\} j\exp\{\pm j\beta z\} \\ H_x^n, H_y^n, E_z^n &= \{H_x^n(x,y), H_y^n(x,y), E_z^n(x,y)\}\exp\{\pm j\beta z\}. \end{aligned} \tag{1}$$

The factor j describes a $\pi/2$ phase difference between the transverse electric and magnetic fields, i.e., E^t and H^t do not refer to values occurring at the same time, but with a time delay. This becomes obvious when the modal information is extracted. Based on the above scheme, a real-variable FDTD algorithm can be derived, which is much easier to process. If the electric- and magnetic-field components are defined on a Yee-like 2-D suppressed staggered grid, then the discretized Maxwell's equations read

$$\begin{aligned} H_x^{n+1}(i,j) &= H_x^n(i,j) - \frac{\Delta t}{\mu} \cdot \left\{ \frac{E_z^n(i,j+1) - E_z^n(i,j)}{\Delta y} - \beta E_y^n(i,j) \right\} \\ H_y^{n+1}(i,j) &= H_y^n(i,j) - \frac{\Delta t}{\mu} \cdot \left\{ \frac{E_z^n(i,j) - E_z^n(i+1,j)}{\Delta x} - \beta E_x^n(i,j) \right\} \\ H_z^{n+1}(i,j) &= H_z^n(i,j) - \frac{\Delta t}{\mu} \cdot \left\{ \frac{E_y^n(i+1,j) - E_y^n(i,j)}{\Delta y} - \frac{E_x^n(i,j+1) - E_x^n(i,j)}{\Delta y} \right\} \\ D_x^{n+1}(i,j) &= D_x^n(i,j) + \Delta t \cdot \left\{ \frac{H_z^n(i,j+1) - H_z^n(i,j)}{\Delta y} + \beta H_y^n(i,j+1) \right\} \\ D_y^{n+1}(i,j) &= D_y^n(i,j) + \Delta t \cdot \left\{ \frac{H_z^n(i,j) - H_z^n(i+1,j)}{\Delta x} + \beta H_x^n(i,j+1) \right\} \\ D_z^{n+1}(i,j) &= D_z^n(i,j) + \Delta t \cdot \left\{ \frac{H_y^n(i+1,j) - H_y^n(i,j)}{\Delta x} - \frac{H_x^n(i,j+1) - H_x^n(i,j)}{\Delta y} \right\} \end{aligned} \tag{2}$$

where Δt, Δx, and Δy are the time step and space steps in the x- and y-directions, respectively. The central finite difference scheme is used to discretize the space along the x- and y-directions, as well as in the time axis t. It is obvious that now only a 2-D process is required with a truly 2-D grid. The anisotropic dielectric properties can be handled easily; using the tensor $\bar{\bar{\varepsilon}}$ to represent the permittivity within any waveguide, which has a reflection symmetry about the z-axis

$$\bar{\bar{\varepsilon}} = \begin{pmatrix} \varepsilon_{i,j}^{xx} & \varepsilon_{i,j}^{xy} & 0 \\ \varepsilon_{i,j}^{yx} & \varepsilon_{i,j}^{yy} & 0 \\ 0 & 0 & \varepsilon_{i,j}^{zz} \end{pmatrix}. \tag{3}$$

Therefore, the electric field is given by

$$\begin{bmatrix} E_x(i,j) \\ E_y(i,j) \\ E_z(i,j) \end{bmatrix} = \bar{\bar{\varepsilon}}^{-1} \begin{bmatrix} D_x(i,j) \\ D_y(i,j) \\ D_z(i,j) \end{bmatrix} \tag{4}$$

where $\bar{\bar{\varepsilon}}^{-1}$ is defined as

$$\bar{\bar{\varepsilon}}^{-1} = \begin{pmatrix} \varepsilon_{i,j}^{xx} & \varepsilon_{i,j}^{xy} & 0 \\ \varepsilon_{i,j}^{yx} & \varepsilon_{i,j}^{yy} & 0 \\ 0 & 0 & \varepsilon_{i,j}^{zz} \end{pmatrix}^{-1} = \begin{pmatrix} a_{i,j}^{xx} & a_{i,j}^{xy} & 0 \\ a_{i,j}^{yx} & a_{i,j}^{yy} & 0 \\ 0 & 0 & a_{i,j}^{zz} \end{pmatrix}. \tag{5}$$

If a tensor of the form given in (5) operates on a vector, both the x- and y-components are needed to evaluate the x- or y-components. However, these components are defined at different locations. We adopt the second-order spatial interpolation scheme [15] that averages the four neighboring components as follows:

$$\begin{aligned} E_x(i,j) &= a_{i,j}^{xx} D_x(i,j) \\ &\quad + 1/4\Big(a_{i+1,j-1}^{xy} D_y(i+1,j-1) \\ &\qquad + a_{i+1,j}^{xy} D_y(i+1,j) + a_{i,j-1}^{xy} D_y(i,j-1) \\ &\qquad + a_{i,j}^{xy} D_y(i,j) \Big). \end{aligned} \tag{6}$$

Since the error introduced in the finite-differencing scheme is of second order, the above interpolation will not introduce any lower order error terms. The condition for stability is given by

$$\nu \Delta t \le \frac{1}{\sqrt{\delta x^{-2} + \delta y^{-2} + (\beta/2)^2}}. \tag{7}$$

In the 2-D-FDTD field simulation, Berenger's perfectly matched layer (PML) absorbing-boundary condition [7]–[8], [18] is implemented on the sidewalls of the problem domain to simulate the open microstrip structure.

Choosing the propagation constant and then exciting the system with a time-domain impulse provides the correct results only at the frequency at which this propagation constant is valid. For any β, we can get N modes with different associated frequencies ω_k $(k = 1, \ldots, N)$. The fields at any position are obtained by superposition of those N modes

$$A(i,j) = \sum_{k=1}^{N} a_k(i,j)\cos(\omega_k t + \phi_{A,k}). \tag{8}$$

The phase shift $\phi_{A,k}$ is an arbitrary value; only the relative phase shifts between the fields are meaningful. During the simulation, the source excites all the modes; this step is then repeated for different propagation constants to obtain the dispersion curve for that particular mode in a broad range of frequency.

Once the fields are obtained, the current and voltage values are calculated from their definitions as

$$i = \oint_c \mathbf{H} \cdot d\mathbf{l} \tag{9}$$

$$v = \int \mathbf{E} \cdot d\mathbf{l} \tag{10}$$

where the contour path for v extends from a defined voltage reference point (usually a ground plane) to the transmission line and c is the transverse contour of a microstrip line. Thus, current and voltage are linear functions of the fields. If I and V represent the current and voltage vectors, then they are the superposition of current and voltage eigenvectors having the same characteristic constant, at different frequencies

$$I = \sum_{k=1}^{N} I_k \cos(\omega_k t + \phi_{i,k}) \tag{11}$$

$$V = \sum_{k=1}^{N} V_k \cos(\omega_k t + \phi_{v,k}). \tag{12}$$

Unlike the static case, the voltage concept in a full-wave model is ambiguous [11]–[12]. As shown in [10] and also observed in this study, the voltage distribution based on the traditional definition under the wide microstrip is not uniform at high frequencies. It is well known that, in microstrip structures, current and transient power have physical meanings, while voltage does not. Instead of arbitrarily choosing a line integral as the voltage, the line-mode voltage matrix is derived by solving the following linear equations [12]–[13]:

$$\left.\begin{aligned} P_k &= \frac{1}{2} V_k^T \bullet I_k \\ 0 &= V_l^T \bullet I_m (l \neq m) \end{aligned}\right\}, \qquad k, l, m = 1, \ldots, N. \tag{13}$$

In (13), P_k is the power flow of the kth mode (modal power flow) and V_k and I_k are voltage and current eigenvectors. Since the modal power flow and the total z-directed current are both uniquely determined quantities, this definition has a clearer physical meaning. The modal power, voltage, and current eigenvectors satisfy the following relationship:

$$[\mathbf{P}] = \frac{1}{2} [\mathbf{V}]^T \cdot [\mathbf{I}] \tag{14}$$

where $[\mathbf{P}]$ is a diagonal matrix built from modal power. $[\mathbf{V}]$ and $[\mathbf{I}]$ are voltage and current eigenvector matrices. The definition of modal power P_k is given by

$$P_k = \int\int (\mathbf{E}_{t,k} \times \mathbf{H}_{t,k}) \cdot d\mathbf{s}. \tag{15}$$

$\mathbf{E}_{t,k}$ and $\mathbf{H}_{t,k}$ are modal transverse fields for the kth mode, which is the real number under this scheme. Unfortunately, this scheme is memory consuming since all the fields in the simulation domain are recorded along the time axis in order to allow subsequent decoupling of the modes. Alternatively, the total transient power $p(t)$ is computed and recorded during simulation

$$p(t) = \int\int (\mathbf{E}_t \times \mathbf{H}_t) \cdot d\mathbf{s}. \tag{16}$$

As mentioned earlier, the electromagnetic fields are superposition of the normal modes at different frequencies. Through this definition, the power is not the superposition of the modal powers; rather, there are N^2 terms, including N modal power. The total power can still be expressed as follows:

$$\begin{aligned} p(t) = &\sum_{k=1}^{N} P_k \cos(2\omega_k t + \phi_{p,k}) \\ &+ \sum_{i=1}^{N} \sum_{j=1,\, j\neq i}^{N} P_{ij} \Big(\cos\big((\omega_i + \omega_j)t + \phi_{ij,+}\big) \\ &\qquad + \cos\big((\omega_i - \omega_j)t + \phi_{ij,-}\big) \Big) \end{aligned} \tag{17}$$

where P_{ij} is defined as

$$P_{ij} = \int\int (\mathbf{E}_{t,i} \times \mathbf{H}_{t,j}) \cdot d\mathbf{s}, \qquad \text{for } i \neq j$$

for the cross term of the power, and $\phi_{ij,+}$ and $\phi_{ij,-}$ are the phase summation and substraction of original two phases. The introduction of the $2\omega_k$ factor in the first term of (17) is due to the $\pi/2$ phase difference between the transverse electric and magnetic fields. The second term on the right-hand side is very small. If i and j refer to different modes at a given frequency, they will be equal to zero as a result of reciprocity [13]. Here, i and j refer to different modes at different frequencies for the same propagation constant. However, the modal configuration change is small in a narrow frequency band. In fact, the existence of this term will not affect our final result when we apply the high-resolution signal-processing techniques to extract the modal information.

Thus, during the FDTD field simulation, the power flux $p(t)$ and current $i(t)$ through each microstrip line are computed and recorded. In this manner, the memory requirement is very small. For comparison, the voltages based on (10) are also obtained.

B. Calculation of Eigenvectors by ESPRIT Algorithm

Once the time-domain simulation has been performed, the frequency-domain information must be retrieved and separated from the noise. The noise arises mainly from the numerical error and the mode formation process. The extraction can be done via Fourier transformation; however, this extraction of the modal information tends to be time consuming. Since the modes are rapidly shaped in the 2-D cross section of waveguide structures, we can apply signal-processing techniques to extract the information in the frequency domain effectively. Here, the ESPRIT algorithm [5] is adopted because of its robustness for data containing additive white noise.

ESPRIT is based on the following data model:

$$x(t) = \sum_{i=1}^{d} a_i(\omega_i) e^{j\omega_i t} + n(t) \tag{18}$$

where ω_i and a_i are the frequency and complex amplitude of the ith modes, d is the total number of modes, and $n(t)$ denotes additive white Gaussian noise. In discretized space, the above equation becomes

$$\begin{aligned} x(k) &= \sum_{i=1}^{d} a_i(\omega_i) e^{j\omega_i k\Delta t} + n(k) \\ &= \sum_{i=1}^{d} a_i(\omega_i) e^{j(\omega_i \Delta t)k} + n(k). \end{aligned} \tag{19}$$

If the data sequence can be described by this ideal model and the number of sampling points $n > 2d + 1$, ESPRIT can resolve each mode exactly. As shown previously, the time-domain field simulated by the 2-D-FDTD corresponds to this model, i.e., for any specific propagation constant β, there are N modes with different ω_i and a_i. Also, there are numerical errors, which can be treated as additive white noise. Hence, the ESPRIT algorithm can extract modal information including the dispersive characteristics and modal templates. The algorithm is applied to the recorded power, current, and voltage of each microstrip line. The modal power, current, and voltage eigenvectors at different frequencies can be extracted in this manner. Consequently, using a scheme based on the 2-D-FDTD ESPRIT algorithms, the voltage and current eigenvectors associated with each propagation mode are extracted. However, as mentioned in [10], the ESPRIT algorithm will not perform well at low frequency in a 3-D-FDTD simulation. In the case under study, acceptable resolution is attained only after longer simulation. This can be attributed to the slow-mode formation process and to the use of a white Gaussian noise at the start of the simulation. Unlike the 3-D-FDTD algorithm, this scheme offers more flexibility in the choice of the time step or mesh size.

C. Extraction of Equivalent-Circuit Parameters

The determination of the equivalent-circuit parameters associated with a transmission line is critical for circuit simulation. Today, full-wave characterization of high-speed circuits has become more commonplace and important in the design process. Here we present a new extraction algorithm based on the theory developed above.

Consider a general multiconductor transmission-line structure with N conductors. For a quasi-TEM mode of propagation, the structure can be considered as a guided wave and can be described by a distributed circuit. The voltage and current on the transmission lines satisfy the generalized frequency-dependent telegrapher's equation

$$\begin{aligned} -\frac{d}{dz} V(z,\omega) &= j\omega \mathbf{L}(\omega) I(z,\omega) \\ -\frac{d}{dz} I(z,\omega) &= j\omega \mathbf{C}(\omega) V(z,\omega) \end{aligned} \tag{20}$$

where $I(z,\omega)$ and $V(z,\omega)$ are current and voltage vectors. $\mathbf{L}(\omega)$ and $\mathbf{C}(\omega)$ are inductance and capacitance matrices, respectively. In this analysis, the loss is neglected. The current and voltage on each line in the time domain can be calculated from the electromagnetic fields by the 2-D-FDTD simulation. This equation is modified for every mode, in which case, a phase shift is introduced. $V(z,\omega) = V(\omega)\exp(j\beta z)$ and $I(z,\omega) = I(\omega)\exp(j\beta z)$, where $V(\omega)$ and $I(\omega)$ are the voltage and current eigenvectors. The following equations are obtained [19]:

$$\begin{aligned} \beta(\omega) V(\omega) &= \omega \mathbf{L}(\omega) I(\omega) \\ \beta(\omega) I(\omega) &= \omega \mathbf{C}(\omega) V(\omega). \end{aligned} \tag{21}$$

The modal information in the frequency domain can be extracted from the ESPRIT algorithm. For an N-line system, we need to excite the system N times with different values of β to get N propagation modes at a fixed frequency. After defining the matrices as

$$\begin{aligned} \mathbf{V}(\omega) &= \begin{bmatrix} [V(\omega)]_1 & [V(\omega)]_2 & \cdots & [V(\omega)]_N \end{bmatrix} \\ \mathbf{I}(\omega) &= \begin{bmatrix} [I(\omega)]_1 & [I(\omega)]_2 & \cdots & [I(\omega)]_N \end{bmatrix} \end{aligned} \tag{22}$$

the frequency-dependent inductance $\mathbf{L}(\omega)$ and capacitance $\mathbf{C}(\omega)$ matrices can be obtained using

$$\mathbf{L}(\omega) = \frac{1}{\omega} \mathbf{V}(\omega) \cdot \mathrm{diag}(\beta_i) \cdot \mathbf{I}(\omega)^{-1} \tag{23}$$

$$\mathbf{C}(\omega) = \frac{1}{\omega} \mathbf{I}(\omega) \cdot \mathrm{diag}(\beta_i) \cdot \mathbf{V}(\omega)^{-1} \tag{24}$$

where $\beta_i (i = 1, 2, \ldots N)$ are the propagation constants associated with the N modes at frequency ω. $\mathbf{V}(\omega)$ and $\mathbf{I}(\omega)$ are voltage and current eigenvector matrices; in this manner, the inductance and capacitance matrices are expressed with eigenvalues β_i, voltage, and current eigenvectors. Although they are derived from the quasi-TEM model, they are valid for the full-wave analysis of interest. However, the voltage eigenvectors should be defined by power–current relationships. If we extract the frequency-dependent inductance $\mathbf{L}(\omega)$ and capacitance $\mathbf{C}(\omega)$ matrices at a frequency ω using the above equations, we must find the N propagation constants β_i $(i = 1, \ldots, N)$ associated with the frequency of interest. This can be done through curve fitting or other interpolation methods from the dispersion relation obtained from the 2-D-FDTD and ESPRIT algorithms. The algorithms are run several times for different propagation constant β; for each run, N different frequencies associated with different modes can be obtained. Next, the curve-fitting method is applied; the magnitude of the current and voltage for different modes at a given frequency can be obtained in the same manner.

For the structure we study, there can be two types of characteristic impedances—the total characteristic impedance and the modal characteristic impedance [16]. The modal characteristic impedance could be useful for studying the nature of hybrid-mode propagation on multiconductor transmission-line systems. On the other hand, total characteristic impedance could be useful for circuit design. The modal characteristic impedances are defined as the ratio between the corresponding elements of the $\mathbf{V}(\omega)$ and $\mathbf{I}(\omega)$ matrices, i.e.,

$$Z_{lk}^{m} = V_{lk}/I_{lk} \tag{25}$$

TABLE I
EIGENVECTORS FOR SYMMETRIC COUPLED LINES

modes	even	odd
frequency(GHz)	25.2	28.3
current eigenvectors	(1,0.997-j0.001)	(1,-0.987-j0.004)
voltage eigenvectors	(1,0.998-j0.001)	(1,-0.984-j0.012)
phase difference between current and voltage	1.578	1.582
normalized equivalent voltage eigenvectors	(0.927-j0.019 , 0.920-j0.015)	(0.938-j0.01 , -0.938+j0.01)

for the kth mode and lth conductor. In [9], the authors give another definition of impedance that allocates the power flow to individual strips. As shown in [10] and also observed by us, there are some discrepancies in the extracted model characteristic impedances by these two definitions, which may be caused by the reasons mentioned in [21] and [22]. In the following calculation, (25) is utilized to compute the modal characteristic impedances. The total characteristic impedance is determined in the matrix form $\mathbf{Z^t}$ given by

$$\mathbf{V^t} = \mathbf{ZI^t} \tag{26}$$

where $\mathbf{V^t}$ and $\mathbf{I^t}$ are arbitrary total vector and current vector, respectively. Therefore, the total characteristic impedance matrix will be given by [16]

$$\mathbf{Z} = \mathbf{VI^{-1}}. \tag{27}$$

Consequently, dispersion characteristics, current and voltage eigenvectors, $\mathbf{C}$ and $\mathbf{L}$ matrices, and impedance parameters—required for a complete circuit description of the system—are directly defined in this context.

The new algorithm is summarized in the following three steps.

Step 1) The fields are simulated using 2-D-FDTD for a specific propagation constant. The total transient power and current on each transmission line are recorded.

Step 2) The modal information is extracted using ESPRIT (The above two steps are repeated N_t times in order to interpolate the modal information over a large frequency range.)

Step 3) The frequency-dependent equivalent-circuit parameters are extracted based on the given equations.

III. NUMERICAL RESULTS

Numerical examples are used to verify this new scheme. Although this method can be used to analyze arbitrary waveguiding structures, such as generalized microstrip line on an inhomogeneous anisotropic substrate or structures with continuous permittivity profiles along the lateral coordinate [20], here, only some planar structures from open literature, where comparable, are available and studied. In all examples, a Gaussian pulse, located underneath the first microstrip line, is used as the excitation; this insures the excitation of all the modes. In the first example, a symmetric coupled transmission-line structure used in a MIC [14] is analyzed. The strips are 0.05-mm thick, 0.3-mm wide, and are separated by 0.3 mm. The dielectric slab is 0.25-mm thick and has a relative dielectric constant ϵ_r of 4.5. The total simulation domain consists of 60 × 30 cells. There are two known modes: the even mode (with eigenvector $[1, 1]$) and the odd mode (with eigenvector $[1, -1]$). The extracted current and voltage eigenvectors for $\beta = 1000$ m^{-1} are shown in Table I. The values are normalized with respect to those on the first line. Fourier transformation fails to distinguish these two modes based on the same data. Note that the equivalent

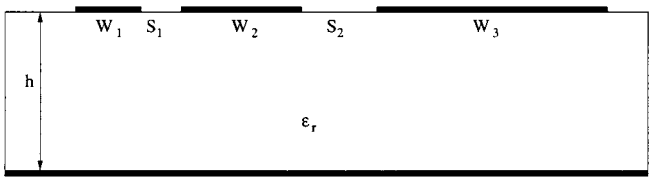

Fig. 1. Geometry of a general three-line coupled microstrip line. $h = 0.635$ mm, $W_1 = 0.3$ mm, $S_1 = 0.2$ mm, $W_2 = 0.6$ mm, $S_2 = 0.4$ mm, $W_3 = 1.2$ mm, and $\epsilon_r = 9.8$.

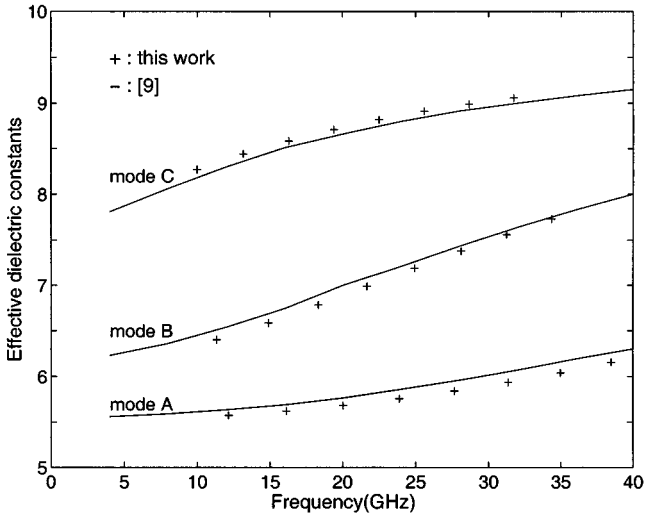

Fig. 2. Effective dielectric constants for the three modes in the three-line structure from Fig. 1.

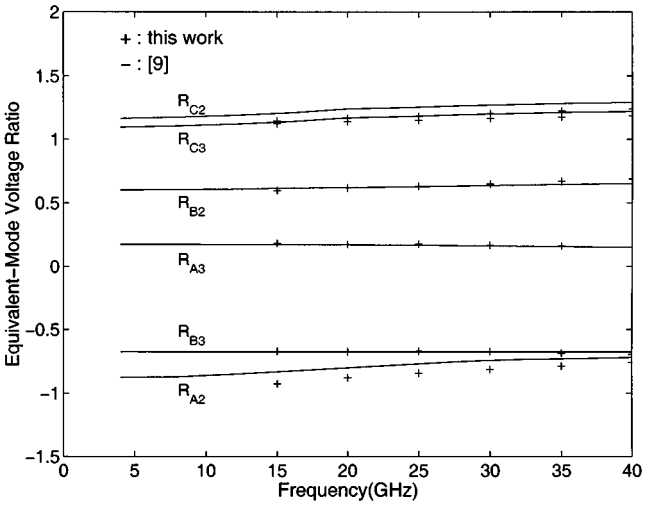

Fig. 3. Equivalent voltage eigenvector matrix elements. The three eigenvectors are $[1, R_{A2}, R_{A3}]$, $[1, R_{B2}, R_{B3}]$, and $[1, R_{C2}, R_{C3}]$.

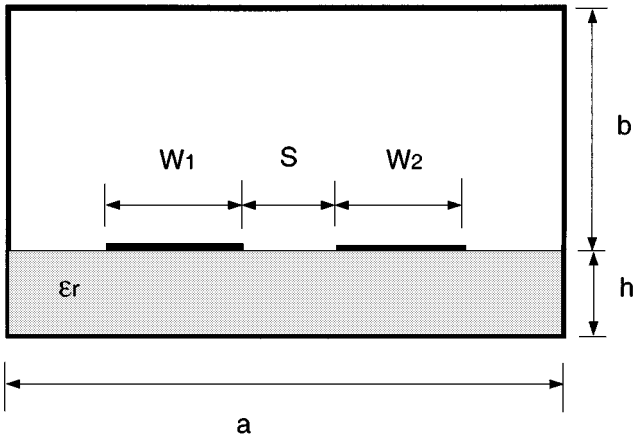

Fig. 4. Cross section of a shield coupled microstrip line. $\epsilon = 4.0$, $h = 1.0$ mm, $b = 4.0$ mm, $W_1 = W_2 = 2.0$ mm, and $S = 1.0$ mm.

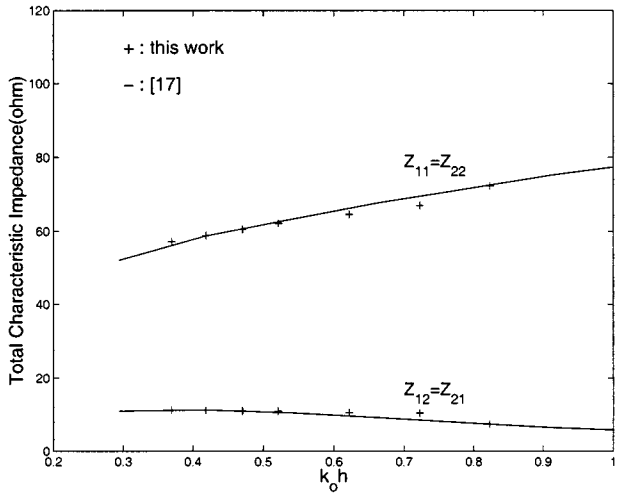

(a)

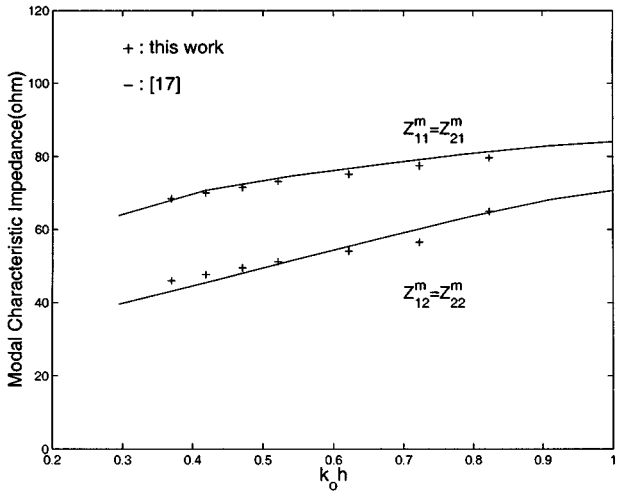

(b)

Fig. 5. (a) Total characteristic impedances for the coupled line. (b) Modal characteristic impedances for the coupled line.

voltage computed using the power–current definition is a bit smaller than that from direct extraction. This can be understood from our FDTD scheme in which we simulate the open structure while keeping the simulation domain as small as possible.

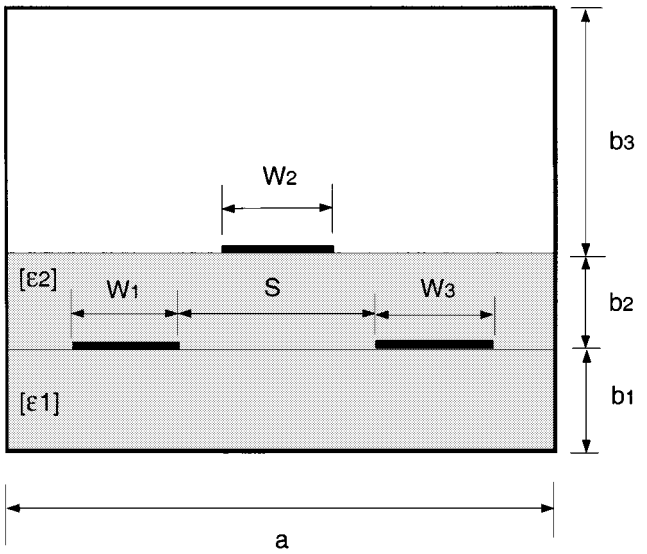

Fig. 6. Cross section of a dual-plane triple microstrip line. $\epsilon_{x1} = \epsilon_{x2} = 9.4\epsilon_0$, $\epsilon_{y1} = \epsilon_{y2} = 11.6\epsilon_0$, $\epsilon_{z1} = \epsilon_{z2} = 9.4\epsilon_0$, $a = 10.0$ mm, $b_1 = b_2 = 1.0$ mm, $b_3 = 4.0$ mm, $W_1 = W_2 = W_3 = 1.0$ mm, and $S = 2.0$ mm.

This leads to an underestimation of the total power flow when the power is computed over the cross section. In fact, when the simulation domain increases, the two solutions do converge. As mentioned earlier, the $\pi/2$ phase shift between the current and voltage values comes from the definition of the fields in (1). Also, for the extraction of modal power, the contribution from the second term of (17) is negligible. This holds for other examples, i.e., the eigenvectors experience negligible change within a narrow frequency band. Thus, the calculation of the eigenvectors for different propagation constants based on the interpolation method gives good approximation. In fact, this procedure can be simplified with the assumption that eigenvectors in a narrow frequency band can be regarded as constants.

The second structure analyzed is the asymmetric three-line coupled microstrip system shown in Fig. 1. The simulation domain consists of 60×30 cells. The effective dielectric constant is generated from the dispersion curve and is shown in Fig. 2. The results are compared with those used in [9], and good agreement is observed. Fig. 3 shows the equivalent modal voltage ratios. Once again, very good agreement is observed between the two results. The results is also at good agreement with those in [10], where 3-D-FDTD is used. Simulation here only requires 300 kB in memory and takes a few minutes in ten simulations for the interpolation on a DEC personal workstation (500-MHz Alpha 21164 processor). The post-processing using the ESPRIT algorithm takes only seconds. At very low frequency, data extraction is slower, yet the ESPRIT algorithm can still extract the parameters by using subsequent simulation data. At low frequencies, mode formation is slower and the needed ESPRIT-type behavior is not achieved until sufficient simulation time has elapsed. This phenomenon is also observed in [10]. Such limitation can be overcome by extending the simulation time or through the use of a coarser FDTD cell.

In our third example, we consider a lossless shield coupled microstrip line shown in Fig. 4. This example was chosen to show the accuracy of this technique. The simulation domain

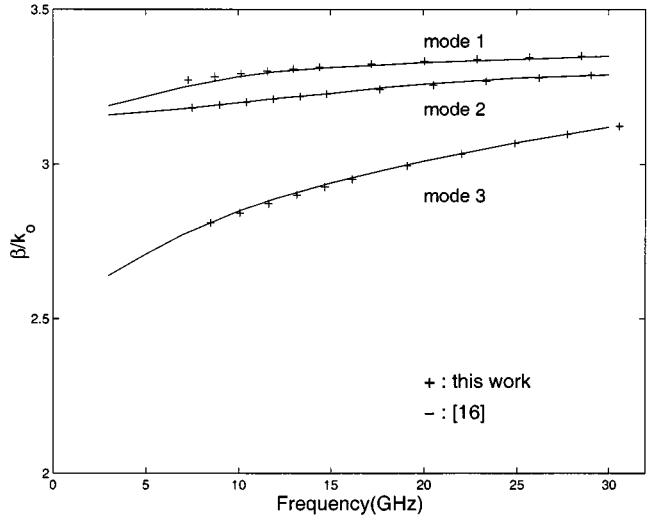

Fig. 7. Normalized propagation constants for the dual-plane triple microstrip line.

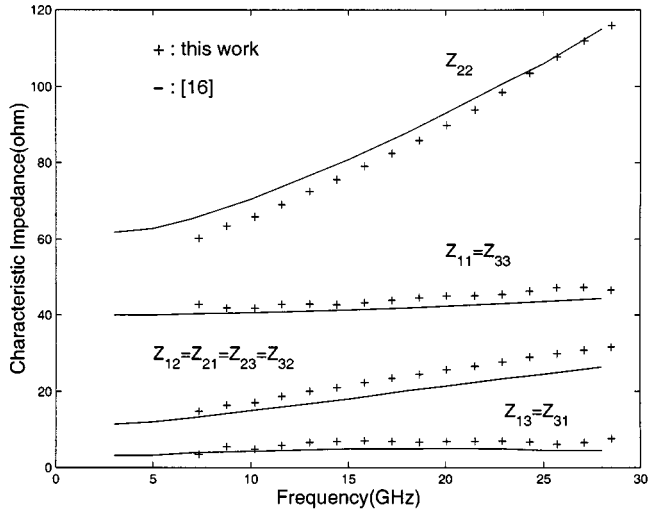

Fig. 8. Total characteristic impedances for the dual-plane triple line.

consists of 40 × 20 cells. It took seconds for each iteration on the aforementioned DEC workstation. Two types of characteristic impedances have been plotted on Fig. 5. The results are compared with those of vector finite-element method (VFEM) and spectral-domain method (SDM) reported by [17]. Very good agreement is seen between the two results. In [16], an efficient finite-element method (FEM) method have been applied for this example. However, their results do not agree very well with those in [17].

The final structure to be analyzed is a dual-plane triple microstrip line on an anisotropic substrate, as shown in Fig. 6. The simulation domain consists of 40 × 24 cells. Dispersion curves for the first three modes are shown in Fig. 7. The results are in very good agreement with those in [16] and [20]. The total characteristic impedances are shown in Fig. 8. The numerical results show that the reciprocity relation, i.e., $Z^t_{ij} = Z^t_{ji}$, is satisfied, although no assumptions of symmetry are used in the simulation. The modal characteristic impedances are

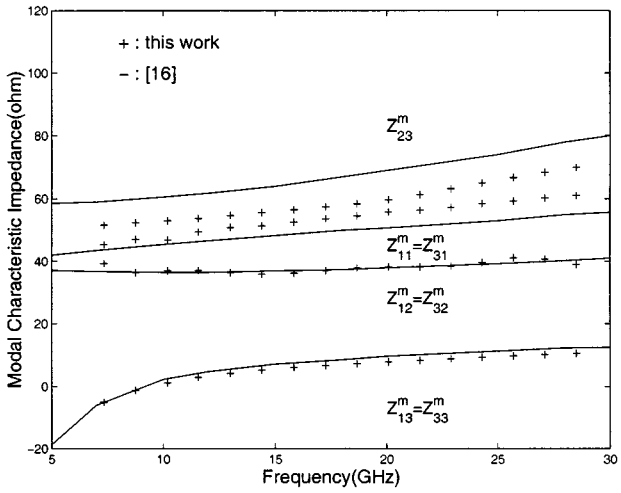

(a)

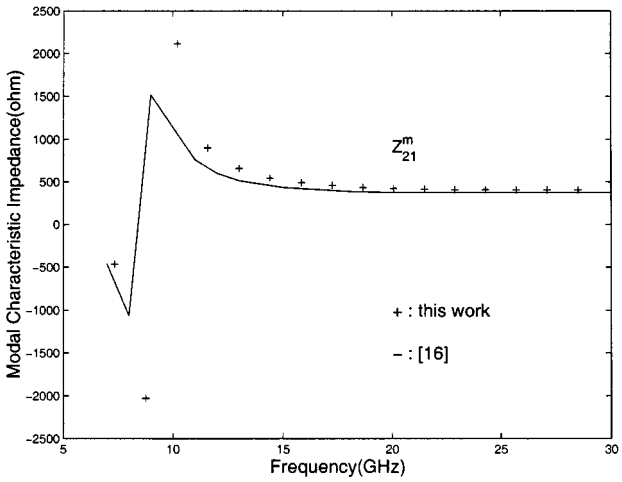

(b)

Fig. 9. Modal characteristic impedances for the dual-plane triple line. (a) Z^m_{11}, Z^m_{12}, Z^m_{13}, Z^m_{23}, Z^m_{31}, Z^m_{32}, and Z^m_{33}. (b) Z^m_{21}.

shown in Fig. 9. Based on our technique, mode 2 is always $[1, 0, -1]$. Considering the symmetry of the structure, there should be mode $[1, 0, -1]$. Thus, Z^m_{22} is not defined, unlike that in [16]. Simulation for this structure only required 250 kB in memory and takes around 3 min on the aforementioned DEC workstation.

IV. Conclusion

A new full-wave analysis method based on 2-D-FDTD and signal-processing techniques is presented for the analysis of waveguide structures in lossless substrates. From a 2-D-FDTD simulation, multimode dispersive modal parameters are easily obtained by using the ESPRIT algorithm. These parameters include the voltage and current eigenvector matrices. A new algorithm is applied to extract the frequency-dependent equivalent-circuit parameters. Good agreement with 3-D-FDTD simulations have been observed for only a fraction of the CPU time and memory requirements. Future work will address the inclusion of substrate loss effects into this approach.

REFERENCES

[1] T. Dhaene and D. De Zutter, "CAD-oriented general circuit description of uniform coupled lossy dispersive waveguide structure," *IEEE Trans. Microwave Theory Tech.*, vol. 40, pp. 1545–1559, July 1992.

[2] J. Zhao and Z. F. Li, "A time-domain full-wave extraction method of frequency-dependent equivalent circuit parameters of multiconductor interconnection lines," *IEEE Trans. Microwave Theory Tech.*, vol. 45, pp. 23–31, Jan. 1997.

[3] S. Xiao, R. Vahldieck, and H. Jin, "Full wave analysis of guided wave structure using a novel 2-D FDTD," *IEEE Microwave Guided Wave Lett.*, vol. 2, pp. 165–167, May 1992.

[4] S. Xiao and R. Vahldieck, "An efficient 2D FDTD algorithm using real variables," *IEEE Microwave Guided Wave Lett.*, vol. 3, May 1993.

[5] R. Roy, A. Paulraj, and T. Kailath, "ESPRIT—A subspace rotation approach to estimation of parameters of cisoids in noise," *IEEE Trans. Acoust., Speech, Signal Processing*, vol. ASSP-34, pp. 1340–1342, Oct. 1986.

[6] R. Schmidt, "Multiple emitter location and signal parameter estimation," *IEEE Trans. Antennas Propagat.*, vol. 34, pp. 276–280, Mar. 1993.

[7] J. P. Berenger, "A perfectly matched layer for the absorption of electromagnetic waves," *J. Comput. Phys.*, vol. 144, pp. 185–200, Oct. 1994.

[8] W. C. Chew and W. H. Weedon, "3D perfectly matched medium from modified Maxwell's equation with stretched coordinates," *Microwave Opt. Technol. Lett.*, vol. 7, no. 13, pp. 599–604, Sept. 1994.

[9] V. K. Tripathi and H. Lee, "Spectral domain computation of the apparent characteristic impedances and multiport parameters of multiple coupled microstrip lines," *IEEE Trans. Microwave Theory Tech.*, vol. 37, pp. 215–221, Jan. 1989.

[10] Y. X. Wang and H. Ling, "Multimode parameter extraction for multiconductor transmission lines via single-pass FDTD and signal-processing techniques," *IEEE Trans. Microwave Theory Tech.*, vol. 46, pp. 89–96, Jan. 1998.

[11] K. D. Marx, "Propagation modes, equivalent circuits, and characteristic terminations for multiconductor transmission lines with inhomogeneous dielectrics," *IEEE Trans. Microwave Theory Tech.*, vol. MTT-21, pp. 450–457, July 1973.

[12] G. Cano, F. Medina, and M. Horno, "Efficient spectral domain analysis of generalized multistrip lines in stratified media including thin, anisotropic, and lossy substrates," *IEEE Trans. Microwave Theory Tech.*, vol. 40, pp. 217–227, Feb. 1992.

[13] F. Mesa, G. Cano, F. Medina, and M. Horno, "On the quasi-TEM and full-wave approaches applied to coplanar multistrip on lossy dielectric layered media," *IEEE Trans. Microwave Theory Tech.*, vol. 40, pp. 524–531, Mar. 1992.

[14] R. Mittra, W. D. Becker, and P. H. Harms, "A general purpose Maxwell solver for the extraction of equivalent circuits of electronic package components for circuit simulation," *IEEE Trans. Circuits Syst. I*, vol. 39, pp. 964–973, Nov. 1992.

[15] J. Schneider and S. Hudson, "The finite-difference time-domain method applied to anisotropic material," *IEEE Trans. Antennas Propagat.*, vol. 41, pp. 994–999, July 1993.

[16] M. S. Alam, M. Koshiba, K. Hirayama, and Y. Hayashi, "Hybrid-mode analysis of mutilayered and multiconductor transmission lines," *IEEE Trans. Microwave Theory Tech.*, vol. 25, pp. 205–211, Feb. 1997.

[17] G. W. Slade and K. J. Webb, "Computation of characteristic impedance for multiple microstrip transmission lines using a vector finite element method," *IEEE Trans. Microwave Theory Tech.*, vol. 40, pp. 34–40, Jan. 1992.

[18] A. P. Zhao, J. Juntunen, and A. V. Raisanen, "Generalized material-independent PML absorbers for the FDTD simulation of electromagnetic waves in arbitrary anisotropic dielectric and magnetic media," *IEEE Microwave Guided Wave Lett.*, vol. 8, pp. 52–54, Feb. 1998.

[19] S. Amari, "Capacitance and inductance matrices of coupled lines from modal powers," *IEEE Trans. Microwave Theory Tech.*, vol. 41, pp. 146–150, Jan. 1993.

[20] K. Radhakrishnan and W. C. Chew, "Full-wave analysis of multiconductor transmission lines on anisotropic inhomogeneous substrates," *IEEE Trans. Microwave Theory Tech.*, vol. 47, pp. 1764–1770, Sept. 1999.

[21] L. Wiemer and R. H. Jansen, "Reciprocity related definition of strip characteristic impedance for muticonductor hybrid-mode transmission lines," *Microwave Opt. Technol. Lett.*, vol. 1, pp. 22–25, Mar. 1988.

[22] G. T. Lei, G. W. Pan, and B. K. Gilbert, "Examination, clarification, and simplification of modal decoupling method for multiconductor transmission lines," *IEEE Trans. Microwave Theory Tech.*, vol. 43, pp. 2090–2100, Sept. 1995.

Feng Liu received the B.S. degree in physics from Peking University, Beijing, China, in 1990, the M.S. degree from Northwestern University, Evanston, IL, in 1995, and is currently working toward the Ph.D. degree in electrical and computer engineering at the University of Illinois at Urbana-Champaign.

In 1996, he joined the Graduate School, University of Illinois at Urbana-Champaign. He is currently with Synopsys Inc., Mountain View, CA. His research is focused on high-speed circuit modeling, signal integrity analysis, and efficient simulation of package interconnects.

José E. Schutt-Ainé (S'86–M'86–SM'98) received the B.S. degree from the Massachusetts Institute of Technology (MIT), Cambridge, in 1981, and the M.S. and Ph.D. degrees from the University of Illinois at Urbana-Champaign (UIUC), in 1984 and 1988, respectively.

From 1981 to 1983, he was an Application Engineer with the Hewlett-Packard Microwave Technology Center, Santa Rosa, CA, where he was involved with transistor modeling. During his graduate studies at UIUC, he held summer positions at GTE Network Systems, Northlake, IL. In 1989, he joined the faculty of the Electromagnetic Communication Laboratory, UIUC, where he is currently an Associate Professor of electrical and computer engineering. His interests include microwave theory and measurements, electromagnetics, high-frequency circuit design, and electronic packaging.

Ji Chen (M'99) received the B.Eng. degree in electrical engineering from the Huazhong University of Science Technology, Wuhan, China, in 1989, the M.Eng. degree from McMaster University, Hamilton, ON, Canada, in 1994, and the Ph.D. degree from the University of Illinois at Urbana-Champaign, in 1998, all in electrical engineering.

From 1998 to 2001, he was a Staff Engineer with the Personal Communications Research Laboratories, Motorola Inc., Harvard, IL. Since 2001, he has been with the Department of Electrical and Computer Engineering, University of Houston, Houston, where he is currently an Assistant Professor. His research interests are in the area of VLSI interconnects modeling, bioengineering, and channel modeling for wireless communications.